Deposition and patterning of diamondlike carbon as antiwear nanoimprint templates

S. Ramachandran, L. Tao, T. H. Lee, S. Sant, L. J. Overzet, M. J. Goeckner, M. J. Kim, G. S. Lee, and W. Hu[a)]
Department of Electrical Engineering, The University of Texas at Dallas, Richardson, Texas 75083-0688

(Received 14 July 2006; accepted 21 September 2006; published 30 November 2006)

In this work, antiwear nanoimprint templates were made by depositing and patterning diamondlike carbon (DLC) films on Si and quartz. A capacitively coupled plasma enhanced chemical vapor deposition (PECVD) system was configured to deposit 100 nm–1 μm thick DLC films on Si and quartz substrates. These films were characterized with Raman spectroscopy, electron energy loss spectroscopy, atomic force microscopy, nanoindentation, contact angle measurements, and optical transmission measurements. The rf power and pressure of the PECVD process were varied to obtain uniform coating of DLC films with smooth surface (~0.2 nm rms), low surface energy (~40 mJ/m^2), and high hardness (~22 GPa). The resulting films' wear resistance is more than three times better than quartz. The DLC films were patterned by nanoimprint lithography using polymethylmethacrylate (PMMA) followed by CF_4 plasma etch. Thermal nanoimprint tests with DLC templates were performed in PMMA. Atomic force microscopy measurements indicated excellent pattern-transfer fidelity and template-polymer separation. © *2006 American Vacuum Society.* [DOI: 10.1116/1.2363409]

I. INTRODUCTION

After almost a decade of research and improvement, nanoimprint lithography (NIL) is beginning to catch the attention of the semiconductor industry as a potential postoptical lithography solution at and below the dynamic random access memory 45 nm half pitch.[1] Moreover, NIL is very promising for the manufacturing of future nanotechnology products, since no other lithography can offer such ultrahigh resolution with high throughput and low cost. However, there are still a number of problems to be solved for NIL to be a practical cost-effective solution, including the difficulties of defect-free fabrication of 1× templates, template lifetime, and overlay.[1] The cost of a template is estimated to be about 1.5 times that of current photomasks.[2] These expensive templates are commonly made of Si and quartz and then coated with an antiadhesion monolayer such as fluorinated silanes.[3] Both the coating layer and the nanostructured template material can suffer from serious damage after a number of imprint cycles, especially in case of hot embossing technique.[4] Currently, there is no effective method to repair damaged templates so wearing damage shortens the template life span and increases manufacturing costs.

One way to alleviate this problem is to use a harder template material for better wear resistance and an extended lifetime. Diamond[5,6] and SiC (Refs. 7 and 8) have been explored to make imprint templates. However, diamond is expensive and grows slowly while SiC is opaque to UV. Diamondlike carbon (DLC) also known as hard amorphous carbon (*a*-C), or hydrogenated amorphous carbon (*a*-C:H), is well researched in the last decades as a common protective optical and tribological coating material. Recently, DLC was investigated as an antistick coating for imprint templates because of its low surface energy.[9] However, DLC has other important properties such as high wear resistance, high corrosion resistance, low coefficient of friction, good biocompatibility, and UV transparency. These interesting properties make DLC an ideal material for nanoimprint templates, not only as an antistick coating. In this article, we report the deposition and patterning of DLC films for imprint templates that offer high wear resistance and robust antistick surface.

II. EXPERIMENT

The DLC films were grown in a capacitively coupled reactor using a mixture of argon and methane (CH_4) as precursor, as shown in Fig. 1. It consists of two electrodes, one at the top and the other at the bottom, with a grounded electrode in the center. Such a configuration allows the independent usage of either the top or the bottom electrode to create the plasma and by removing the center electrode, it is possible to achieve independent control over the ion energies by biasing both the top and bottom electrodes. rf power at 13.56 MHz was capacitively coupled to the lower electrode through an *L*-type matching network. Typical deposition conditions were rf power of 100–450 W resulting in a dc bias between −100 and −400 V, pressure of 30–100 mTorr, and deposition rate of ~10 nm/min. Using this plasma enhanced chemical vapor deposition (PECVD) process, DLC films with thicknesses from 100 nm up to 1 μm were deposited onto 0.5 mm thick Si and quartz wafers.

The structural properties of the DLC film were studied with Raman spectroscopy, using a Jobin Yvon Labram high-resolution micro-Raman spectrometer with laser excitation at 633 nm. The spectra were collected at multiple points on a single sample and fitted with disordered carbon (*D*-peak) and graphitic carbon (*G*-peak) Gaussians using a commercial

[a)]Electronic mail: walter.hu@utdallas.edu

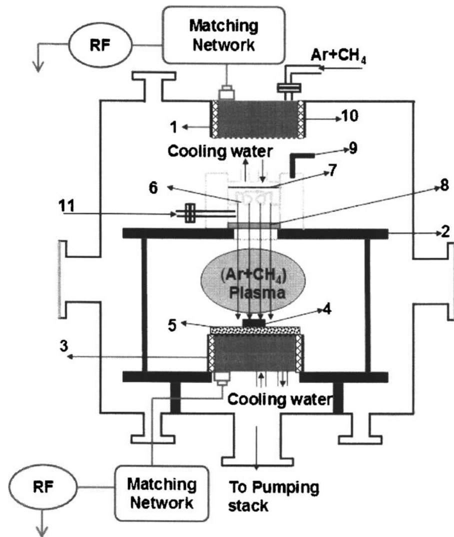

FIG. 1. Schematics of DLC deposition PECVD system. Parts illustration for the PECVD system: (1) upper showerhead electrode, (2) center grounded electrode, (3) lower biased electrode, (4) sample, (5) thermal insulator, (6) infrared lamp, (7) aluminum reflector, (8) quartz window for lamp protection, (9) electrical connection for lamp, (10) Teflon insulators, and (11) purge for lamp protection.

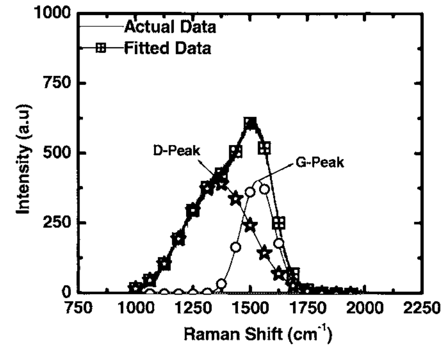

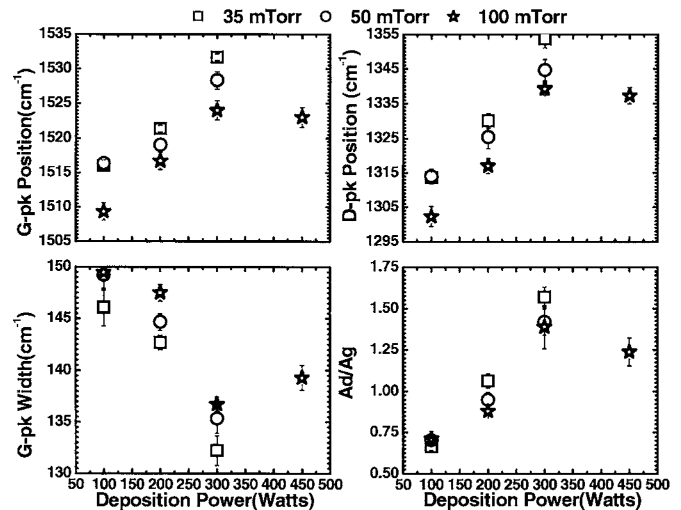

FIG. 2. Raman spectra of DLC films: (a) a typical Raman spectra fitted with disordered carbon peak (*D* peak) and graphite peak (*G* peak); the spectrum corresponds to a film deposited at 300 W rf power and 50 mTorr chamber pressure. (b) Positions and widths of *G* peak and *D* peak derived from spectra fitting, as a function of deposition bias power and pressure.

graphing software. The mean values and deviations of the Raman fitting parameters were calculated and used to obtain the trends exhibited as a function of the deposition conditions. For electron-energy-loss spectroscopy (EELS) analysis, the cross-sectional samples were prepared for transmission electron microscope (TEM). Data were collected using a Gatan ENFINATM detection electron-energy-loss spectrometer attached to a JEOL-2100F TEM. Contact angle for water and ethylene glycol were measured on a Ramè Hart manual contact angle goniometer and surface energies were calculated using a two-liquid method.[10] The optical measurements were performed on an n&k analyzer 1200RT/Iris 200, and reflectance and transmission measurements were performed for wavelengths between 190 and 900 nm. Surface roughness of the DLC films were measured using atomic force microscopy (AFM). Hardness of the DLC films was measured using a Hysitron nanoindentor[11] with 75 nm wide diamond tips and maximum loads of 100 μN. Wear tests were performed on the same nanoindentor using a 150 nm diameter diamond tip at normal loads of 40 μN to scan $5 \times 5\ \mu m^2$ areas. The wear regions were imaged *in situ* and the average depths of each wear region as well as the volume of material removed were determined.

DLC coated Si and quartz substrates were spin coated with 300–800 nm thick polymethylmethacrylate (PMMA). Nanoimprint was performed at a temperature of 160 °C and pressure of 60 MPa for 10 min. O_2 plasma in an inductive coupled plasma (ICP) system was used to remove the resist residue. DLC was etched using CF_4 both with and without 5% O_2 addition at pressures between 20 and 60 mTorr, bias power of 50 W, and ICP power of 400 W. After etch, the remaining resist was stripped using acetone. Both the DLC patterns and surface roughness before and after etch were measured using an AFM.

III. RESULTS AND DISCUSSION

A. DLC structural properties

Raman spectroscopy is widely used to characterize the structural properties of *a*-C:H films in part because it allows one to collect valuable data in a simpler fashion.[12] The Raman spectrum of DLC films exhibits a broad feature centered around 1550 cm^{-1}, as shown in Fig. 2(a). That raw spectrum confirms that the film structure is similar to that of DLC and the absence of a sloping photoluminescence background confirms that it is closer to diamondlike *a*-C:H, as opposed to a polymerlike *a*-C:H.[13] In order to quantify the structural variations from their Raman spectra, it is useful to fit the raw spectrum with two Gaussians centered at approximately 1350 and 1580 cm^{-1}. These represent the disorder (*D*) and graphitic (*G*) peaks, respectively, as shown in Fig. 2(a). We note that the absolute *G*-peak position in Fig. 2(b) is always

a little smaller than in similar works but believe that this is not important and due to the excitation wavelength used.[14] Rather than the absolute values, it is the variations in the fitting parameters [G- and D-peak center positions, their widths and area ratios (A_D/A_G)] that enable one to qualitatively estimate changes in the ratio of sp^3 bonded carbon to sp^2 bonded carbon.[15–17] From Fig. 2(b), it can be seen that the G peak moves to higher wave numbers with increasing bias powers, indicating an increase in the percentage of sp^2 bonded carbon in the film. Alternatively, the sp^3 bonding percentage is decreasing with bias power. The decreasing width of the G peak with power in Fig. 2(b) coupled with the increasing area ratio (A_D/A_G) is further evidence of the same. The latter observation is generally explained as a result of an increase in sp^2 cluster sizes.[15] The higher percentage of sp^3 bonds found at lower powers is thought to be a result of higher concentrations of hydrogen in the film.[18] This hydrogen is more effectively removed (sputtered) as the bias power is increased, resulting in increasing sizes for the sp^2 clusters and the motion of the G peak to higher wave numbers. Higher pressures caused reduced sp^2 cluster sizes. The lower G-peak positions and A_D/A_G ratios and higher G-peak widths provide evidence for such a trend. One possible reason for this pressure trend is that the dc self-bias (and ion energy)becomes larger at constant power as the pressure is lowered. This can cause an increased sputter yield of hydrogen from the films at lower pressures even though the power is the same. It should also be noted that the variations with pressure, though consistent, are small compared to the variations with power.

A turnover point was observed between the films deposited at 350 and 450 W at 100 mTorr. The G-peak position falls back slightly to lower wave numbers accompanied by an increase in the width of the G peak and decrease in the A_D/A_G ratio. These trends again indicate an increase in the sp^3/sp^2 fraction in the films (decreasing sp^2 cluster sizes). Unfortunately, it was not possible to carry out the film deposition at 450 W for 35 and 50 m Torr chamber pressures due to electrical problems with the deposition reactor. It is possible that this turnover point is indicative of a transition of the film structure from being predominantly a-C:H to a-C. We were able to perform EELS on a couple of samples as a cross-check of the structural properties (results not shown). The peak around 24 eV in the low loss peak, coupled with the less intense shoulder corresponding to the π^* states near 285 eV, confirmed that these films were not graphitic in nature, and were rather more diamondlike atomic structure.[19–21]

The optical band gap of the films were measured and Fig. 3 contains the transmission spectra for films deposited on quartz at two different bias powers. The optical transmission is inversely proportional to the deposition power. These results support the trends shown by Raman in that the shift of the G peak to higher wave numbers results in films with an increased sp^2 fraction and consequently a lower optical band gap. Unfortunately, the films deposited at the lower bias, though being more transparent, contain a higher fraction of hydrogen and hence are softer. The trade off between the

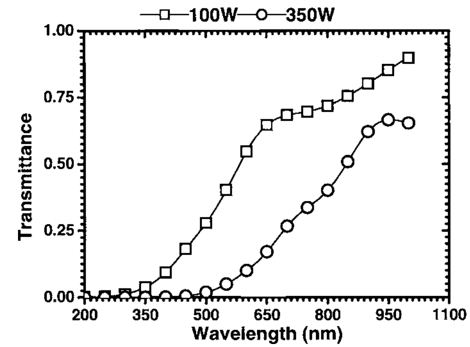

FIG. 3. Transmission spectra for DLC films on quartz substrate. The films were deposited at a chamber pressure of 100 mTorr.

tribological properties and optical band gap is critical in defining the performance of these structures for UV-NIL applications. As seen from Fig. 3, at the typical wavelengths used in UV-NIL processes, the transmissivity of the films are only approximately 10%. Though it is possible to compensate for the loss in transmissivity by increasing the exposure time during pattern transfer, a more practical approach is to optimize the deposition conditions and obtain a balance between the optical and mechanical properties.

The surface energies of the material used as a patterning mold in NIL applications play a crucial role in defining the fidelity of the pattern transfer. Contact angle measurements were performed with water and ethylene glycol, and the polar and dispersive components of the surface energy were calculated using the two-liquid method. The contact angles plotted in Fig. 4 show no significant dependence on the deposition conditions, and the calculated surface energies of as deposited DLC films were in the range of 35–50 mJ/m^2, which should satisfy the requirements for template-polymer separation (also known as demolding process).

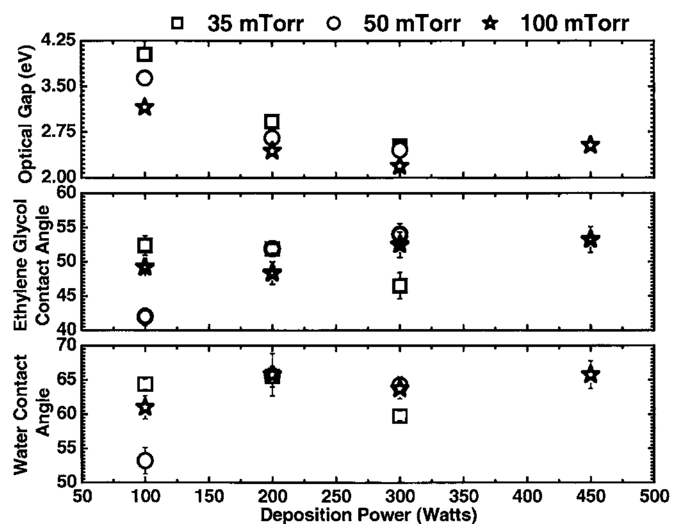

FIG. 4. Optical gap and contact angle of water and ethylene glycol as a function of PECVD bias power and pressure.

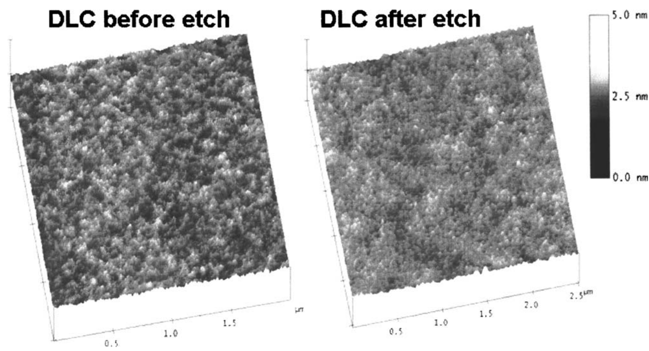

FIG. 5. AFM images of DLC film on Si before and after CF_4 etch. Film deposition was done at 150 mTorr chamber pressure and 350 W deposition power.

TABLE I. Surface energies of DLC films before and after ICP etch.

	Contact angle (°)		Surface energy[a] ($\gamma=\gamma^d+\gamma^p$) (mJ/m^2)		
ICP etch conditions	H_2O	Ethylene glycol	γ^p	γ^d	γ
Before etch	57.0	52.5	45.8	2.9	48.6
CF_4, 20 mTorr	89.5	55.0	1.4	36.6	38.0
CF_4, 60 mTorr	90.0	61.0	2.7	28.0	30.7
CF_4+5% O_2, 20 mTorr	59.0	43.0	32.4	9.7	42.0
CF_4+10% O_2, 20 mTorr	57.0	41.5	34.8	9.1	43.9

[a]Surface energy γ is the sum of γ^d- (dispersion component) and γ^p (polar component).

B. Hardness and wear testing

Our hardness measurements indicated that these DLC films ranged from 18 to 23 GPa and that larger deposition powers resulted in harder films. The DLC templates were found to be about 2 times harder than Si (10.6 GPa) and quartz (9.3 GPa). The abrasive wear of DLC films on Si and quartz were investigated as described in a previous section. Both DLC films showed similar wear depths, 2.00 nm for DLC on quartz and 1.98 nm for DLC on Si, under a force load of 40 μN on a 150 nm diamond tip. For comparison, the wear depth on Si was 3.75 nm and on quartz was 6.39 nm indicating that the wear resistance of a DLC template is 3 times better than quartz and almost 2 times better than Si.

C. DLC template fabrication and imprint testing

DLC films were etched using PMMA as mask with CF_4 gas with and without the addition of 5%–10% O_2 at total flow rates of 40 SCCM (SCCM denotes cubic centimeter per minute at STP), pressures between 20 and 60 mTorr, a bias power of 50 W, and an inductively coupled plasma power of 400 W. The etch rate of DLC was about 75 nm/min and selectivity of PMMA to DLC was about 5:1. A DLC template with 0.5–50 μm features and 75 nm depths was fabricated using this ICP process. The surface roughness before and after etch was measured using AFM, as shown in Fig. 5. The RMS roughness of the DLC film before etch was 0.168 and 0.159 nm after the etch, which proved the etching process did not affect the surface roughness. The surface energy of DLC films before and after etch are shown in Table I. CF_4 etching reduced the DLC surface energy from ~49 mJ/m^2 to between 31 and 44 mJ/m^2 depending on the gas mixture and pressure. The absence of any significant variations in the surface roughness before and after the CF_4 treatment rules it out as a factor causing the change in surface energies. We believe that the change in the surface energy is due to the formation of a thin CF_x film over the *a*-C:H film. In particular, a significant difference in the polar and dispersion components of the surface energy was observed dependent upon the addition of O_2. Since most polymers are polar materials, the polymer-template adhesion strength is mainly determined by the polar component of template surface energy. In this case, a pure CF_4 etch is desired for making antistick template surfaces. These surface energies were stable for more than 10 days and after acetone and isopropyl alcohol rinsing. The robust low energy surface of the DLC template is tunable by the ICP gas setup and voids the need for fragile trichlorosilane antistick coatings. The natural medium surface energy of DLC (~40 mJ/m^2) is perfect for reversal nanoimprint, in which polymer is spin coated on the template and can be used to transfer patterns over topography.[22]

Preliminary thermal imprints were carried out with the patterned DLC template at 165 °C and 60 MPa for 10 min in 400-nm-thick 950 K PMMA. The template-polymer separation was quite easy and polymer did not adhere to the template. Both the template and imprinted PMMA patterns were imaged using AFM, as shown in Fig. 6. Dimensions and depths of the 1 μm lines in the DLC template measured about 1.06 μm and 72.6–79.8 nm, respectively. The geometry of PMMA patterns measured about the same values and proved a good pattern-transfer fidelity.

IV. SUMMARY

DLC films were deposited onto Si and quartz substrate using a PECVD process. They were patterned using nanoimprint and ICP etch to be nanoimprint templates. DLC films and templates were systematically characterized by Raman

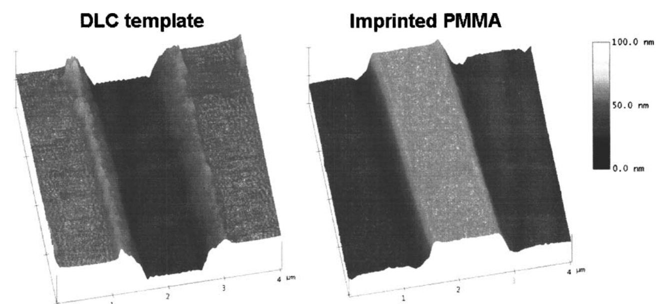

FIG. 6. AFM images of DLC template and imprinted PMMA patterns: (a) etched DLC trenches with 1 μm width and 67 nm depth; (b) 1 μm wide and 67 nm high PMMA lines imprinted at 165 °C and 60 MPa for 10 min. Film deposition was done at 150 mTorr chamber pressure and 350 W deposition power.

spectroscopy, EELS, optical transmission measurement, nanoindentation, AFM, and contact angle measurements. The DLC template has the following properties: (1) confirmed hydrogenated amorphous carbon films, (2) hardness of 18–23 GPa, (3) high wear resistance of more than three times of quartz, (4) robust and tunable low surface energy (35–50 mJ/m^2), (5) 10% transmittance at 300–500 nm wavelengths, and (6) uniform pin-hole free deposition with ~0.16 nm surface roughness. These properties make DLC a suitable template material for longer lifetime and lower cost of ownership than Si or quartz templates.

[1]2005 International Technology Roadmap for Semiconductors, see http://www.public.net/itrs
[2]Webcast: Nanoimprint Lithography, Semiconductor International, 17 December 2005.
[3]T. Bailey, B. J. Choi, M. Colburn, M. Meissl, S. Shaya, J. G. Ekerdt, S. V. Sreenivasan, and C. G. Willson, J. Vac. Sci. Technol. B **18**, 3572 (2000).
[4]R. W. Jaszewski, H. Schift, B. Schnyder, A. Schneuwly, and P. Groning, Appl. Surf. Sci. **143**, 301 (1999).
[5]J. Taniguchi, Y. Tokano, I. Miyamoto, M. Komuro, and H. Hiroshima, Nanotechnology **13**, 592 (2002).
[6]K. A. Lister, S. Thoms, D. S. Macintyre, C. D. W. Wilkinson, J. M. R. Weaver, and B. G. Casey, J. Vac. Sci. Technol. B **22**, 3257 (2004).
[7]P. H. Yin, V. Saxena, and A. J. Stenckl, Phys. Status Solidi B **202**, 605 (1997).
[8]S. W. Pang, T. Tamamura, M. Nakao, A. Ozawa, and H. Masuda, J. Vac. Sci. Technol. B **16**, 1145 (1998).
[9]U.S. Patent No. 20050084804 (pending).
[10]D. K. Owens and R. C. Wendt, J. Appl. Polym. Sci. **13**, 1741 (1969).
[11]Hysitron TriboIndenter, http://www.hysitron.com
[12]M. A. Tamor and W. C. Vassell, J. Appl. Phys. **76**, 6 (1994).
[13]C. Casiraghi, F. Piazza, A. C. Ferrari, D. Grambole, and J. Robertson, Diamond Relat. Mater. **14**, 1098 (2005).
[14]M. Bonelli, A. C. Ferrari, A. Foravanti, A. L. Bassi, A. Miotello, and P. M. Ossi, Eur. Phys. J. B **25**, 269 (2002).
[15]A. C. Ferrari and J. Robertson, Phys. Rev. B **61**, 14095 (2002).
[16]J. Scwan, S. Ulrich, V. Batori, H. Ehrhardt, and S. R. P. Silva, J. Appl. Phys. **80**, 440 (1996).
[17]A. C. Ferrari and J. Robertson, Phys. Rev. B **64**, 075414 (2001).
[18]M. J. Paterson, K. G. Orrman-Rossiter, and S. Bhargava, J. Appl. Phys. **75**, 792 (1994).
[19]L. Ponsonnet, C. Donnet, K. Varlot, J. M. Martin, A. Grill, and V. Patel, Thin Solid Films **319**, 97 (1998).
[20]J. Kulik, Y. Lifshitz, G. D. Lempert, J. W. Rabalais, and D. Marton, J. Appl. Phys. **76**, 5063 (1994).
[21]S. R. P. Silva and V. Stolojan, Thin Solid Films **488**, 283 (2005).
[22]L. R. Bao, X. Cheng, X. D. Huang, L. J. Guo, S. W. Pang, and A. F. Yee, J. Vac. Sci. Technol. B **20**, 2881 (2002).